AIRS Deconvolution and Translation from the AIRS to CrIS IR Sounders

**** DRAFT ****

Howard E. Motteler
L. Larrabee Strow

UMBC Atmospheric Spectroscopy Lab
Joint Center for Earth Systems Technology

February 14, 2017

1 Introduction

Upwelling infrared radiation as measured by the AIRS [1] and CrIS [2, 6] sounders is a significant part of the long term climate record. We would like to treat this information as a single data set but the instruments have different spectral resolutions, channel response functions, and band spans. As a step in addressing this problem we consider the translation of channel radiances from AIRS to standard resolution CrIS.

Translation from AIRS to CrIS involves more that simple resampling. AIRS is a grating spectrometer with a distinct response function for each channel determined by the focal plane geometery, while CrIS is a Michaelson interferometer with a sinc ILS after calibration and corrections. In section 2 we show how to take advantage of our detailed knowledge of the AIRS spectral response functions (SRFs) and their overlap to deconvolve channel radiances to a resolution-enhanced intermediate representation, typically 0.1 cm^{-1}, the approximate resolution of the tabulated AIRS SRFs.

The AIRS to CrIS translation then consists of two steps, deconvolution of the AIRS channel radiances to the intermediate grid, typically 0.1 cm^{-1},

followed by reconvolution to the CrIS user grid. Section 3 gives the details. In section 4 we show how to further improve residuals by adding a statistically based correction.

2 AIRS Deconvolution

The AIRS spectral response functions model channel response as a function of frequency and associate channels with nominal center frequencies. Each AIRS channel i has an associated spectral response function or SRF $\sigma_i(v)$ such that the channel radiance $c_i = \int \sigma_i(v) r(v)\, dv$, where r is radiance at frequency v. The center or peak of σ_i is the nominal channel frequency.

Figure 1 shows a typical subset of AIRS SRFs. Note the significant overlap in the wings. This allows the deconvolution to recover resolution beyond that of the response functions considered individually. The spacing of the AIRS L1b channels is not regular; there are both gaps and close neighbors, side effects of the focal plane geometry. Both the gaps and close neighbors cause problems for a deconvolution. The AIRS L1c channel set [**?**] is a derived product of the 1b set with filled gaps and relatively regular (though still frequency dependent) frequency spacing, and we will use the 1c set here.

Suppose we have n channels and a frequency grid $\vec{v}$ of k points spanning the domains of the functions σ_i. The grid step size for our applications is often 0.0025 cm^{-1}, the kcarta resolution. Let S_k be an $n \times k$ array such that $s_{i,j} = \sigma_i(v_j)/w_i$, where $w_i = \sum_j \sigma_i(v_j)$, that is where row i is $\sigma_i(v)$ tabulated at the grid $\vec{v}$ and normalized so the row sum is 1. If the channel centers are in increasing order S_k is banded, and if they are not too close the rows are linearly independent. S_k is a linear transform whose domain is radiance at the grid $\vec{v}$ and whose range is channel radiances. If r is radiance at the grid $\vec{v}$, then $c = S_k r$ gives a good approximation of the channel radiances $c_i = \int \sigma_i(v) r(v)\, dv$.

In practice this is how we convolve kcarta or other simulated radiances to get AIRS channel radiances. We construct S_k either explicitly or implicitly from AIRS SRF tabulations. The matrix S_k in the former case is large but manageable with a banded or sparse representation.

Suppose we have S_k and channel radiances c and want to find r, that is, to deconvolve c. Consider the linear system $S_k x = c$. Since $n < k$ for the kcarta grid mentioned above this is underdetermined, with infinitely many solutions. We could add constraints, take a pseudo-inverse, consider a new

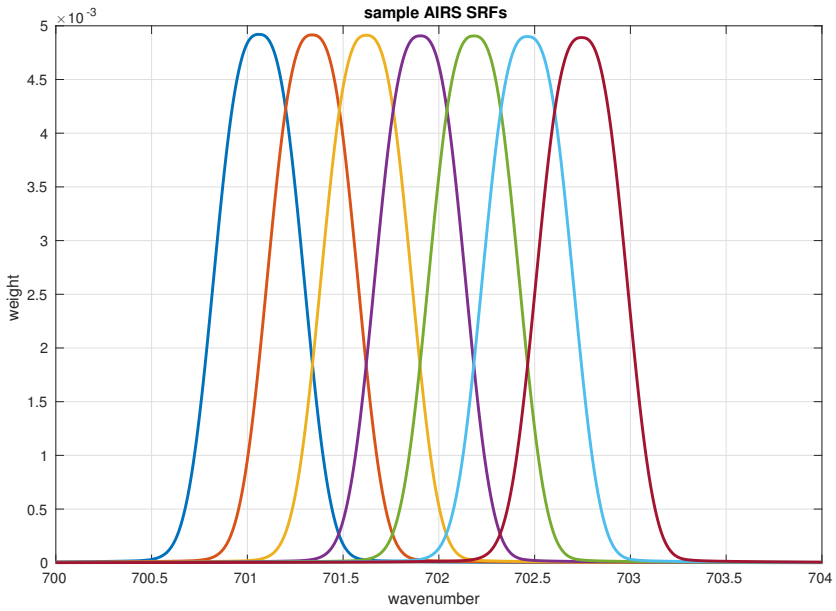

Figure 1: sample adjacent AIRS spectral response functions

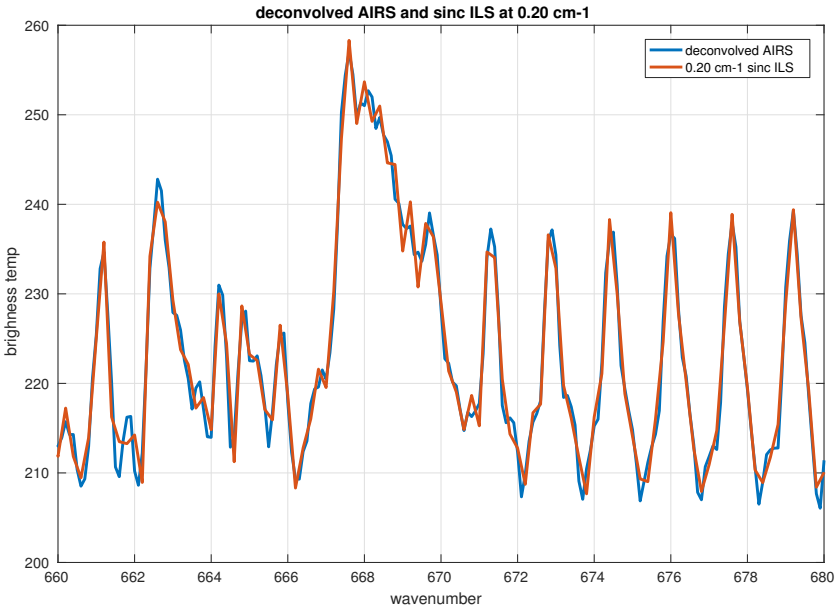

Figure 2: detail of deconvolved AIRS and kcarta 0.0025 cm^{-1} radiances convolved to a sinc ILS at 0.2 cm^{-1}

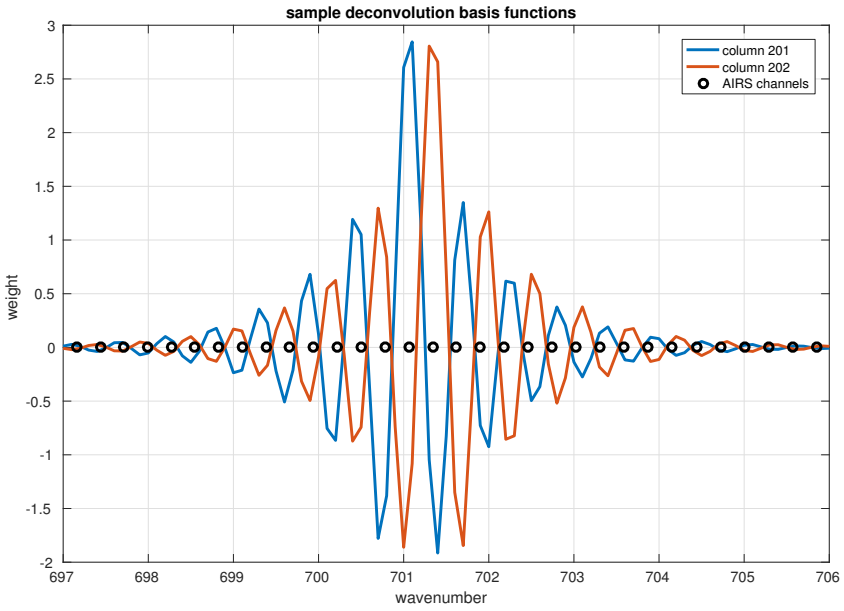

Figure 3: sample basis function for the deconvolved AIRS radiances

matrix S_b with columns tabulated at some coarser grid, or some combination of the above.

For an AIRS to CrIS translation we are mainly interested in the transform S_b with SRFs at an intermediate grid, typically 0.1 cm^{-1}, the approximate resolution of the SRF measurements. Let $\vec{v}_b = v_1, v_2, \ldots, v_m$ be a 0.1 cm^{-1} grid spanning the domains of the functions σ_i. Similar to S_k, let S_b be an $n \times m$ array where row i is $\sigma_i(v)$ tabulated at the $\vec{v}_b$ grid, with rows normalized to 1. If r is radiance at the $\vec{v}_b$ grid, then $c = S_b r$ is still a reasonable approximation of $\int \sigma_i(v) r(v)\, dv$.

Consider the linear system $S_b x = c$, similar to the case $S_k x = c$ above, where we are given S_b and channel signals c and want to find radiances x. Since $n < m < k$, as with S_k the system will be underdetermined but more manageable because m is approximately 40 times less than k. We use a Moore-Penrose pseudoinverse as S_b^{-1}. Then $x = S_b^{-1} c$ gives us deconvolved radiances at the SRF tabulation grid.

The AIRS deconvolution gives a significant resolution enhancement. Figure 2 shows LW detail of deconvolved AIRS together with kcarta radiances convolved directly to a 0.2 cm^{-1} sinc ILS. Figure 3 shows a typical basis function for the AIRS deconvolution, that is, a column of the pseudo-inverse

S_b^{-1}.

3 AIRS to CrIS translation

For the CrIS standard resolution mode the channel spacing is 0.625 cm^{-1} for the LW, 1.25 cm^{-1} for the MW, and 2.5 cm^{-1} for the SW bands. The first step in the AIRS L1c to CrIS translation is to deconvolve the AIRS channel radiances to the 0.1 cm^{-1} intermediate grid, the nominal AIRS SRF resolution. Then for each CrIS band, we

- find the AIRS and CrIS band intersection
- apply a bandpass filter to the deconvolved AIRS radiances to restrict them to the intersection, with a rolloff outside the intersection
- reconvolve the filtered spectra to the CrIS user grid

Translations are validated by comparison with calculated reference truth. For the results presented in this section we start with 49 fitting profiles spanning a significant range of atmospheric conditions [3, 5]. Upwelling radiance is calculated at a 0.0025 cm^{-1} grid with kcarta [4] over a band spanning the AIRS and CrIS response functions. "True AIRS" is calculated from this by convolving the kcarta radiances with AIRS SRFs, and "true CrIS" by convolving kcarta radiances to the CrIS instrument specifications. AIRS is then translated to CrIS to get "AIRS CrIS", and this is compared with true CrIS. This validation assumes perfect knowledge of the AIRS and CrIS instrument response functions and so gives only a lower bound on residuals, and on how well the translations can work in practice. The better we know the response functions, the closer real translations can approach these limits.

Figure 4 shows true CrIS, true AIRS, deconvolved AIRS, and AIRS CrIS. In the first subplot we mainly see the greater fine structure in the deconvolution. The second subplot shows details from 660 to 680 cm^{-1}.

Figures 5, 6, and 7 show the mean and standard deviation of true CrIS minus AIRS CrIS for the 49 fitting profiles, with and without Hamming apodization, for each of the CrIS bands. Figures 8 and 9 summarize the mean and standard deviation of the residuals for Hamming apodized radiances. The residual has a high frequency component with a period of 2 channel steps that is significantly reduced by the apodization. The constant or DC bias

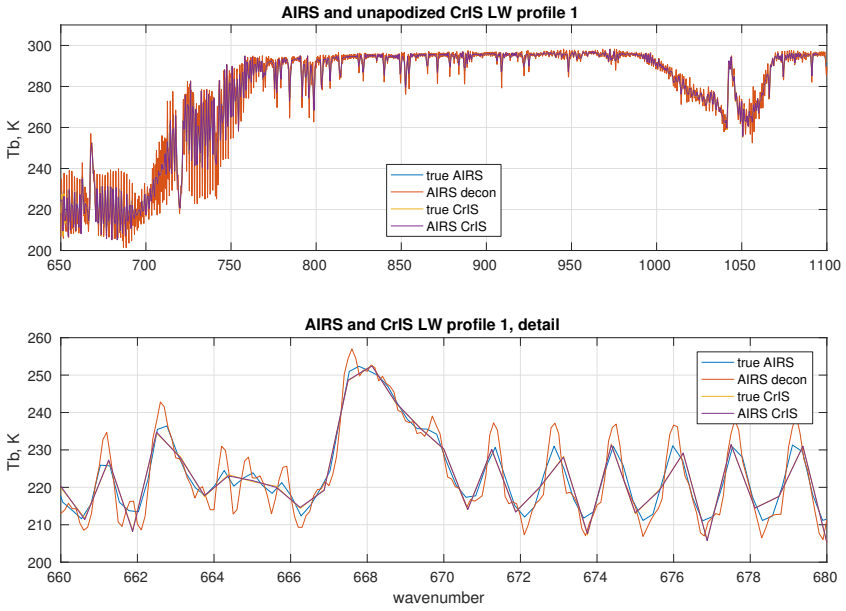

Figure 4: true CrIS, true AIRS, deconvolved AIRS, and AIRS CrIS

(the mean of the residuals over frequency) is close to zero for the apodized residuals: 0.002 K for the LW, −0.005 K for the MW, and 0.001 K for the SW.

Deconvolution works better than interpolation for the AIRS to CrIS translation. We consider two cases. For the first, start with true AIRS and interpolate radiances directly to the CrIS user grid with a cubic spline. For the second, interpolate true AIRS to the 0.1 cm^{-1} intermediate grid with a cubic spline and then convolve this to the use CrIS user grid. Figure 10 shows interpolated CrIS minus true CrIS for the LW band, without apodization. The two-step interpolation works a little better than the simple spline, but both residuals are significantly larger than for the translation with deconvolution. Results for the MW are similar, while the unapodized comparison is less clear for the SW. With Hamming apodization, the residuals with deconvolution are significantly less than interpolation for all three bands.

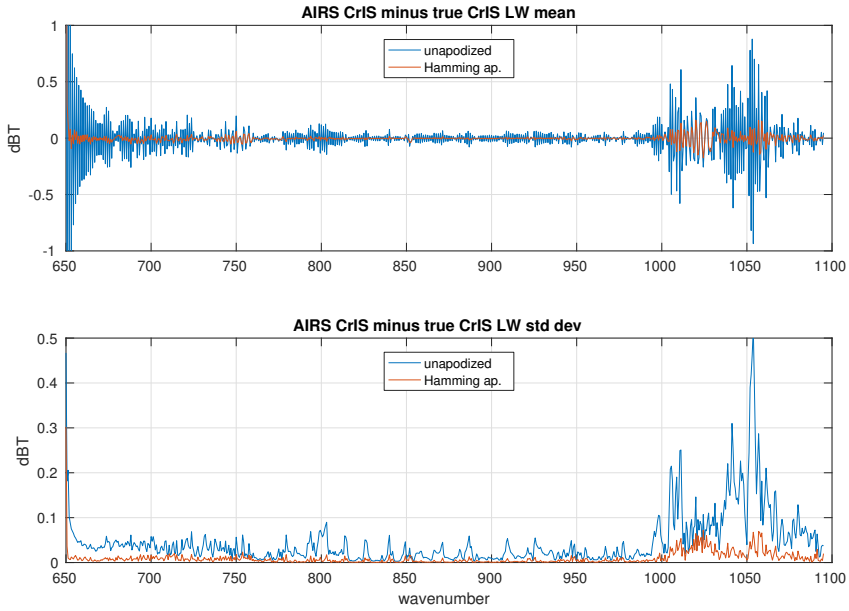

Figure 5: Mean and standard deviation of unapodized and Hamming apodized AIRS CrIS minus true CrIS, for the CrIS LW band

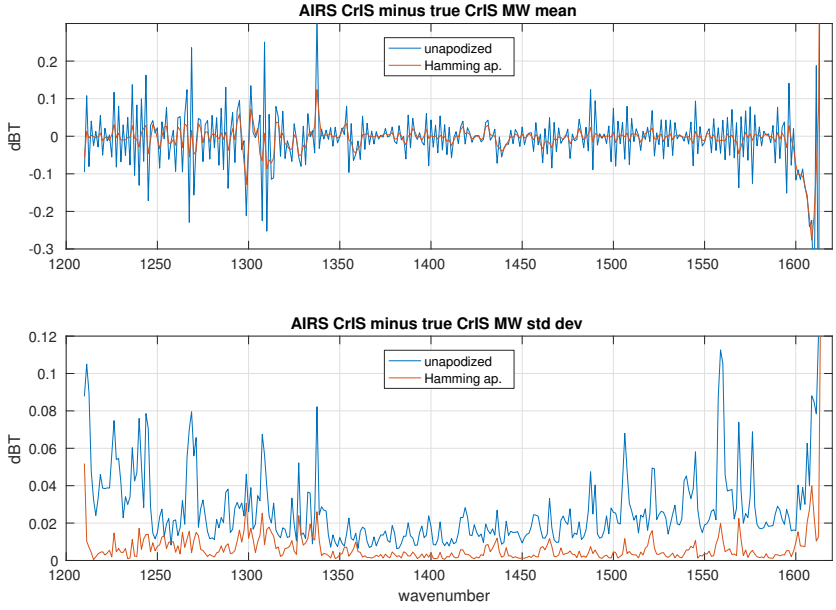

Figure 6: Mean and standard deviation of unapodized and Hamming apodized AIRS CrIS minus true CrIS, for the CrIS MW band

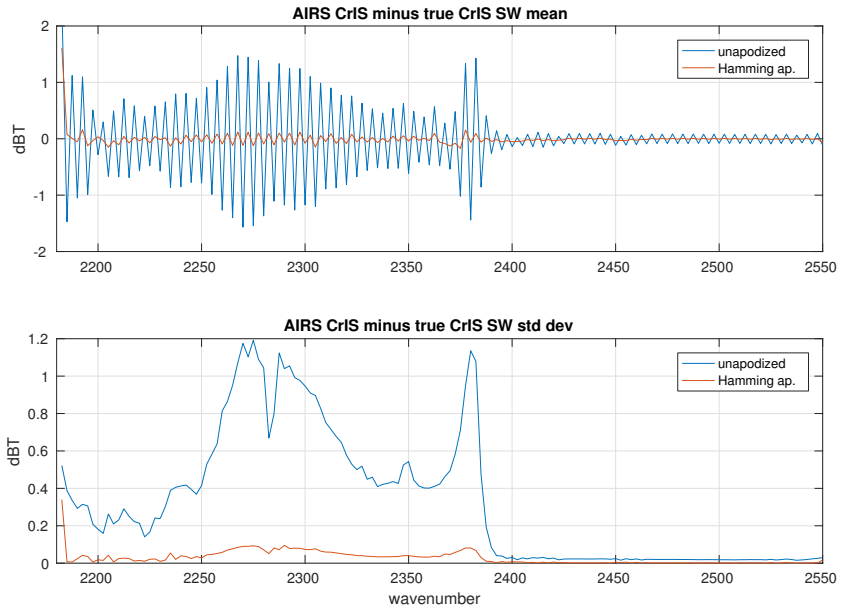

Figure 7: Mean and standard deviation of unapodized and Hamming apodized AIRS CrIS minus true CrIS, for the CrIS SW band

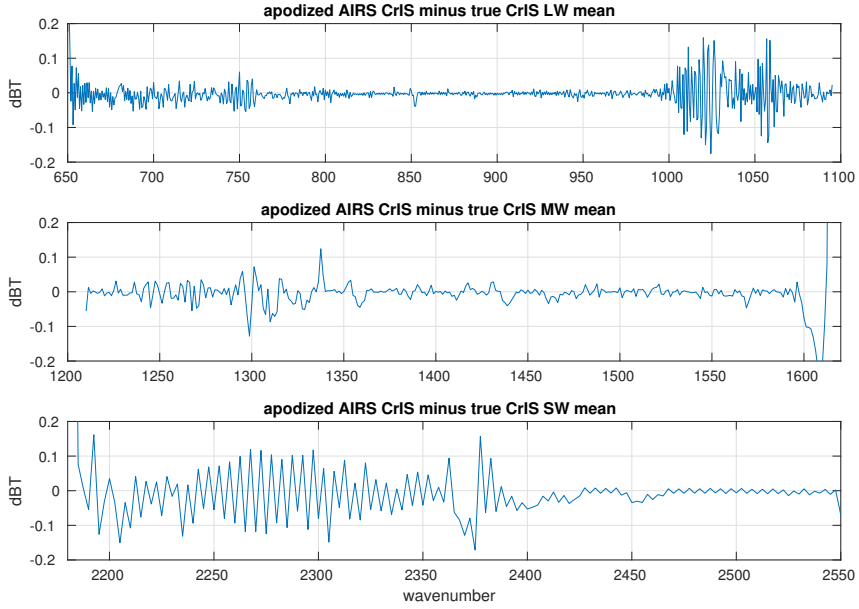

Figure 8: Mean apodized residuals for all three bands

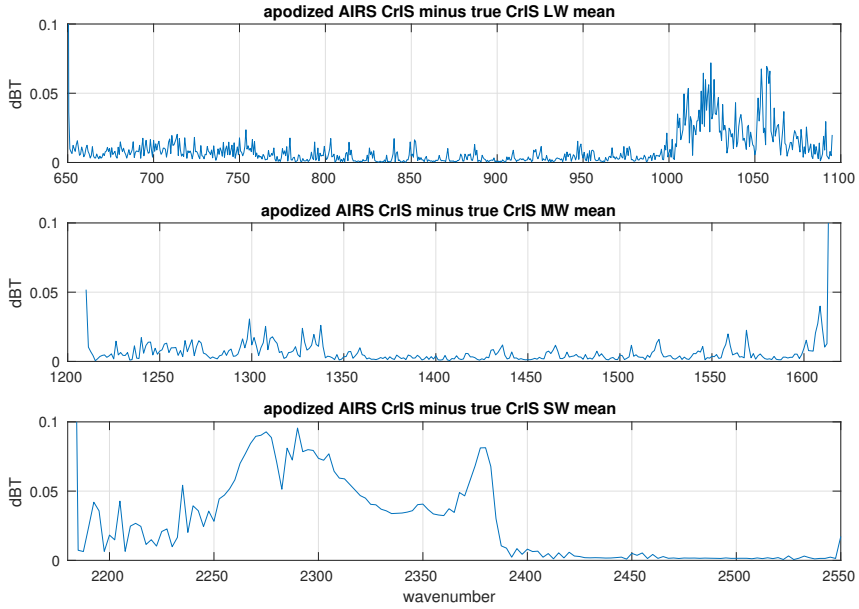

Figure 9: Standard deviation apodized residuals for all three bands

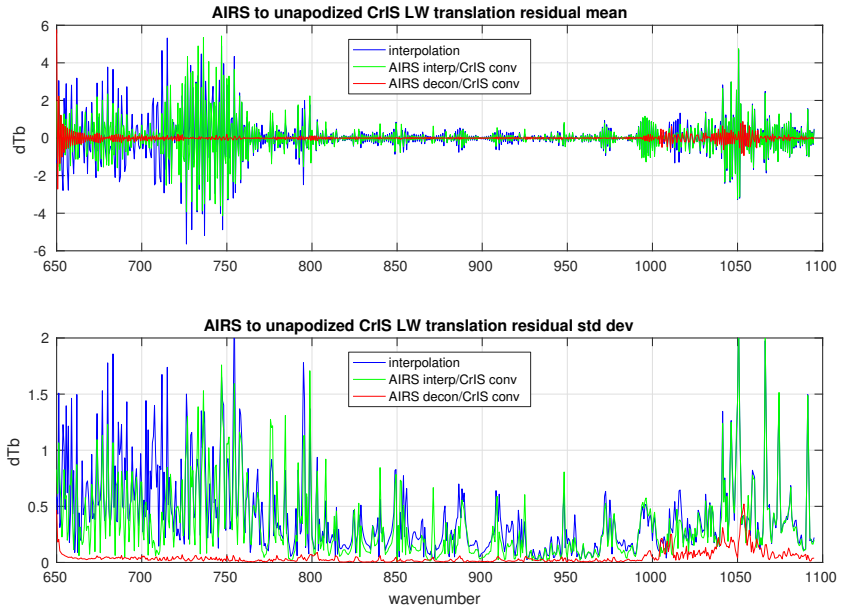

Figure 10: spline interpolation, interpolation with convolution, and deconvolution with convolution for the CrIS LW band

4 Statisitcal Refinement

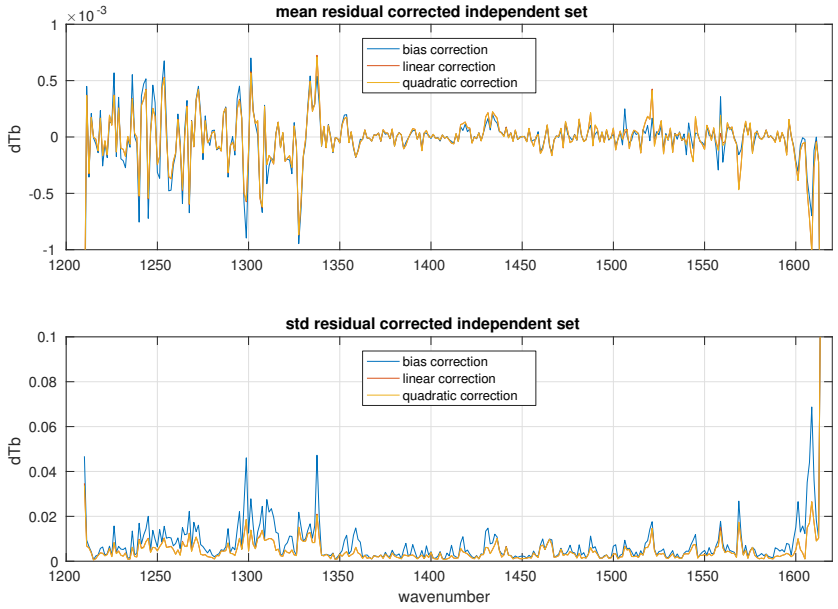

Figure 11: Mean and standard deviation of LW corrected apodized residuals for the independent subset of the 7377 profile set

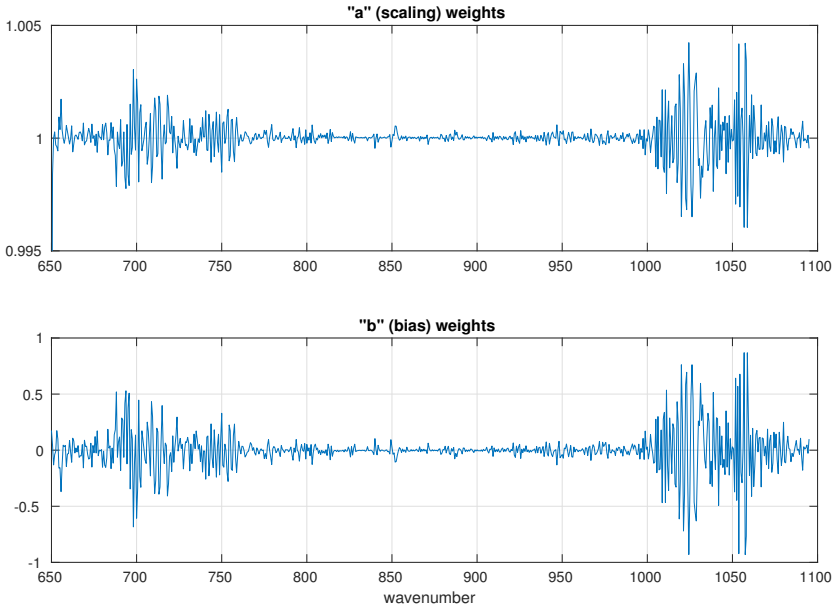

Figure 12: LW a and b weights for the linear correction $ax + b$

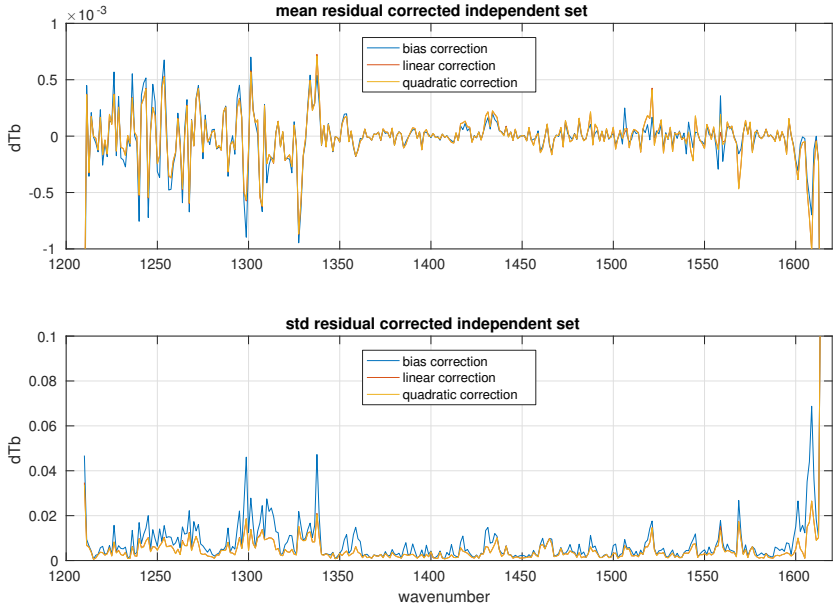

Figure 13: Mean and standard deviation of MW corrected apodized residuals for the independent subset of the 7377 profile set

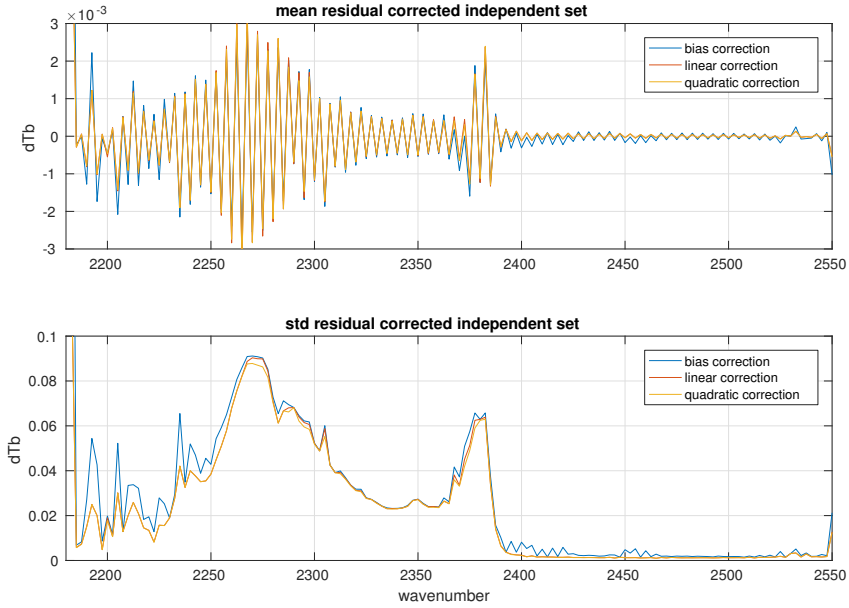

Figure 14: Mean and standard deviation of SW corrected apodized residuals for the independent subset of the 7377 profile set

References

[1] H. H. Aumann, M. T. Chahine, C. Gautier, M. D. Goldberg, E. Kalnay, L. M. McMillin, H. Revercomb, P. W. Rosenkranz, W. L. Smith, D. H. Staelin, L. L. Strow, and J. Susskind. AIRS/AMSU/HSB on the aqua mission: design, science objectives, data products, and processing systems. *IEEE Transactions on Geoscience and Remote Sensing*, 41:253–264, Feb. 2003.

[2] Y. Han, H. Revercomb, M. Cromp, D. Gu, D. Johnson, D. Mooney, D. Scott, L. Strow, G. Bingham, L. Borg, Y. Chen, D. DeSlover, M. Esplin, D. Hagan, X. Jin, R. Knuteson, H. Motteler, J. Predina, L. Suwinski, J. Taylor, D. Tobin, D. Tremblay, C. Wang, L. Wang, L. Wang, and V. Zavyalov. Suomi NPP CrIS measurements, sensor data record algorithm, calibration and validation activities, and record data quality. *Journal of Geophysical Research (Atmospheres)*, 118:12734, Nov. 2013.

[3] L. Strow, S. Hannon, S. De Souza-Machado, H. Motteler, and D. Tobin. An overview of the airs radiative transfer model. *Geoscience and Remote Sensing, IEEE Transactions on*, 41(2):303–313, Feb 2003.

[4] L. Strow, H. E. Motteler, R. G. Benson, S. E. Hannon, and S. D. Souza-Machado. Fast computation of monochromatic infrared atmospheric transmittances using compressed look-up tables. *Journal of Quantitative Spectroscopy and Radiative Transfer*, 59(35):481 – 493, 1998. Atmospheric Spectroscopy Applications 96.

[5] L. L. Strow, S. E. Hannon, S. De-Souza Machado, H. E. Motteler, and D. C. Tobin. Validation of the atmospheric infrared sounder radiative transfer algorithm. *Journal of Geophysical Research: Atmospheres*, 111(D9), 2006. D09S06.

[6] L. L. Strow, H. Motteler, D. Tobin, H. Revercomb, S. Hannon, H. Buijs, J. Predina, L. Suwinski, and R. Glumb. Spectral calibration and validation of the Cross-track Infrared Sounder on the Suomi NPP satellite. *Journal of Geophysical Research (Atmospheres)*, 118:12486, Nov. 2013.